Cleaved fiber optic double nanohole optical tweezers for trapping nanoparticles

Ryan M. Gelfand, Skylar Wheaton, and Reuven Gordon*

Department of Electrical and Computer Engineering, University of Victoria, Victoria British Columbia, Canada
**Corresponding author: rgordon@uvic.ca*

Received August 5, 2014; revised October 8, 2014; accepted October 9, 2014;
posted October 9, 2014 (Doc. ID 220315); published November 6, 2014

We demonstrate the trapping of single 20 and 40 nm polystyrene spheres at the cleaved end of a fiber optic with a double nanohole aperture in gold and without any microscope optics. An optical transmission increase of 15% indicates a trapping event for the 40 nm particle, and the jump is 2% for the 20 nm particle. This modular technique can be used to replace those used with current optical trapping setups that require complicated free space optics and frequent calibration, with one that is modular and requires no free space optics. This simple arrangement with the potential for fiber translation is of interest for future biosensor and optical nano-pipette devices. © 2014 Optical Society of America

OCIS codes: (060.2370) Fiber optics sensors; (140.7010) Laser trapping; (350.4855) Optical tweezers or optical manipulation; (220.4241) Nanostructure fabrication.
http://dx.doi.org/10.1364/OL.39.006415

Fiber optic technology has become an increasingly important component for next generation biosensing devices [1,2]; it is inexpensive, compact, versatile, robust, and commercially mature [3]. With optical biosensor platforms gaining more traction as exhibiting both sensitivity and selectivity [4–6], integrating them with existing technologies will continue to be important. Fiber optics are used as optical elements for Raman probes [7], SPR sensing [8], fluorescent microscopy [9], and *in vivo* spectroscopy [10,11]. Fiber optics have also been used as elements in microfluidic devices for imaging [12] and sensing [13]. The integration of an optical trap/tweezer that can trap biologically relevant nanoparticles, such as proteins, with a fiber optic would add single particle trapping and manipulation to existing fiber based sensing platforms leading to the detection, identification, and observation of single nanoparticles.

Our lab has already shown the trapping of single proteins [14] using a double nanohole [15] (DNH) optical aperture based trap, and this new technology could provide researchers with a tool for working at the single particle limit. Currently, the trapping and single particle interrogation is performed using a free space setup based on an inverted microscope [16]. The transmission through the DNH trap is monitored and an increase in transmission indicates a trapped particle. The trapping is more efficient than that of conventional gradient force tweezers because of self-induced back-action (SIBA) [17] and can therefore trap single nanometer scale biological particles such as DNA [18] and proteins [19] without destroying them. However, the microscope setup is neither portable nor inexpensive and requires maintaining alignment of the optics. By fabricating the DNH trap directly onto the cleaved end of a fiber optic, we provide a portable, low-cost solution that requires no alignment. This device could potentially be used to trap and interrogate single nanoparticles, as a nano-pipette to manipulate the trapped particles and to observe how they interact in different environments.

Two groups have demonstrated trapping of nanoscale [20,21] objects using an aperture fabricated at the end of a fiber optic; however, both relied on a tapered fiber, which adds complicated fabrication steps and makes the fiber more fragile. We demonstrate the trapping of 20 and 40 nm polystyrene (PS) beads onto the flat cleaved end of a fiber optic using a DNH trap, without the need for complicated optics or tapered fiber fabrication techniques.

DNH traps were fabricated onto the cleaved end of SMF 28e Corning Optical Fiber by mounting them onto a clamp that secures the fibers in place and upright and fits into both our focused ion beam (FIB) and SEM, as shown in Fig. 1(a). The fibers have a core region of doped silicon dioxide, which is 8 μm with a cladding region of undoped silicon dioxide, which is 125 μm. This structure produces an optical mode roughly the same diameter as the core region, so it is important for the

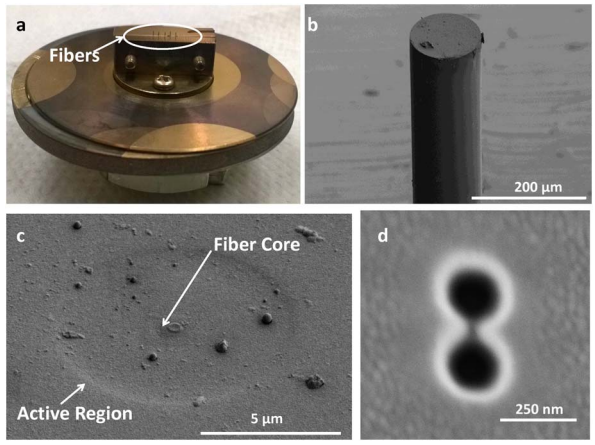

Fig. 1. (a) Fiber mount for processing the ends of fibers in the FIB and SEM; the holder fits five fibers and ensures the tips are pointed toward the source. (b) 30° tilted SEM image of one of the fibers mounted in the sample holder so that the cleaved end can easily be processed. (c) 50° tilted SEM image of the active region of the fiber made visible by the selective buffered HF etching. The unetched center is from that region being undoped because of the manufacturing process of the fiber optic. (d) SEM image of the finished DNH trap milled into the active region of the fiber.

DNH traps to be milled within this area. First the fibers were cleaved using a precision automatic cleaver and then mounted into the holder at 90°, allowing access to the flat active end for processing [Fig. 1(b)]. The fibers were etched for 45 s in a buffered HF solution so the active region is visible [22] with the SEM [Fig. 1(c)]. An e-beam evaporator was then used to deposit 5 nm of titanium and 80 nm of gold followed by a 20 nm angled sputter deposition of gold/palladium so that the tops of the fibers are electrically and thermally connected to the metallic holder. This reduced the effects of charging in both the SEM for imaging and the FIB for accurate milling.

The doped region of the fiber etches more quickly than the undoped, leaving a slight imprint for registration of the core. To achieve the contrast between the etched and unetched regions, the SEM was operated with a low aperture setting and long working distance; in this case 13 mm was used. The stage was tilted to 50° to make the active area more distinct. After confirming the location of the active area, the FIB was used to mill one DNH structure near the center of the active area for each fiber. The gap was 40 ± 2 nm, as measured with the SEM. The diameter of the two annular openings was 180 nm, as shown in Fig. 1(d).

Figure 2 shows a schematic of the measurement setup. The holder fits five fibers at a time and after fabrication they were spliced with an APC/FC connectorized optical patch cable. One fiber was removed and then, with its trap side facing downward, was then mounted onto a grooved plate with soft magnetic clamps which was then mounted to a stage so the fiber can be translated into the liquid containing the analyte. A 980 nm pigtailed diode laser was connected to a polarization controller, which was then connected to the patch cable. For the detection, we measured the transmission through the DNH trap with a standard, inexpensive, large area (7.8 mm diameter) silicon photodetector, whose output was collected using a data acquisition card. A glass slide was attached to the inside of a petri dish, covered, and sealed with paraffin wax to limit evaporation. A droplet with the target analyte was placed on the glass slide through a hole in the top of the container. The petri dish was placed over the photodetector with no lens needed to collect the transmitted signal. The fiber was then lowered into the liquid, as close to the glass slide as possible. Fine stage controls were used to ensure that the delicate DNH trap did not hit the top of the glass slide or the edges of the paraffin wax hole as it was brought near the liquid droplet. The transmission was monitored on an oscilloscope and recorded with a data acquisition card. The DNH traps are polarization sensitive; maximum transmission occurs when the electric field is aligned across the short axis of the gap. A polarization controller was adjusted until the transmission signal was maximized.

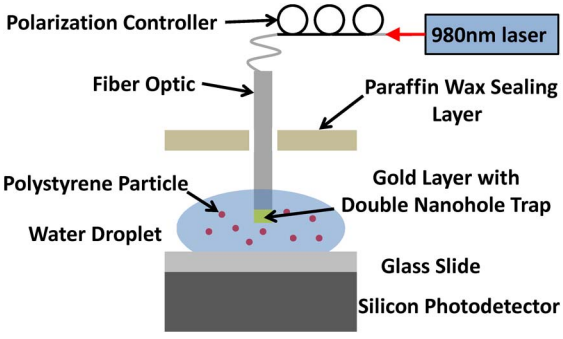

Fig. 2. Schematic of the characterization setup for the fiber based optical trap. A DNH trap milled through gold on the end of a fiber optic is lowered into a droplet of water containing polystyrene particles. Once a single nanoparticle is trapped the transmission through the aperture increases.

The fiber was first inserted into a bead of water containing 0.3% by weight 40 nm spherical PS particles dropped directly over the detector. A 980 nm laser connected through a polarization controller was set to output 5 mW/μm^2 and the transmission was measured with a silicon photodetector. Optical transmission through a subwavelength aperture will increase if the dielectric constant of the aperture increases. By loading the gap of our DNH apertures with a single particle, we increase the dielectric constant of the gap and observe a transmission increase [14]. Figure 3(a) shows a trapping event for a 40 nm PS sphere in water. The 15% signal increase is attributed to the particle filling most of the gap of the DNH structure. Without particles in the solution, no jumps were observed.

For the second experiment we used 20 nm PS spheres suspended in a 0.3% solution by weight, and the laser output was set at 6 mW/μm^2. The experiment was conducted the same way as the first with a different fiber. SEM images confirmed that each of the DNH traps had been milled to within 2 nm of each other. Figure 3(b)

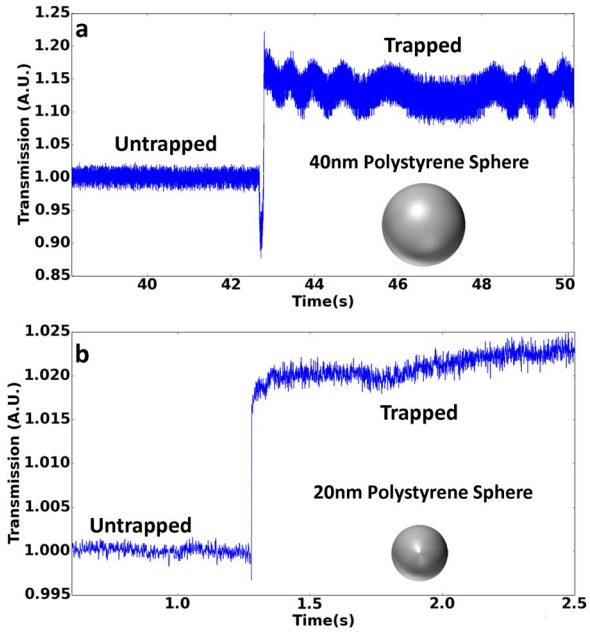

Fig. 3. (a) Trapping event for a 40 nm polystyrene sphere in a DNH on the cleaved end of a fiber optic. The 15% increase in the transmitted light shows a strong trapping event for this DNH. (b) Trapping event for a 20 nm polystyrene sphere in a DNH on the cleaved end of a fiber optic. The 2% jump in the transmitted signal shows a weaker trapping event for this DNH; however, the particle is clearly trapped for a timescale on the order of minutes.

shows the trapping event for a 20 nm sphere; the signal jump is less because the dielectric loading is smaller because of the smaller particle size. The experiment was repeated 10 times with two additional fibers. The signal increases were very similar for each fiber. For the 40 nm spheres, the average transmission increase and standard deviation for the first fiber was $15\% \pm 0.2\%$ and for the second fiber was $14.5\% \pm 0.3\%$. For the 20 nm spheres, the average transmission increase for the first fiber was $2.0\% \pm 0.3\%$ and for the second fiber was $2.4\% \pm 0.3\%$.

If more than one particle were trapped in the gap, we would see multiple transmission jumps in the signal; however, since we have only observed a single jump, we can conclude that only one PS particle is trapped. In addition, the consistency in the step size for a given particle size indicates that we are trapping individual particles and not aggregates. Typically, only a single particle is trapped, which we attribute to the combined effects of steric hindrance and the particles in solution being charged by the surfactant.

As the particle is trapped, the signal root mean squared variation increases because as it vibrates in the trap, because of the Brownian motion, the transmission signal fluctuates. Even with a lower signal jump, we have seen using our conventional free space trapping setup the ability to trap small proteins and even DNA hairpin molecules, so we are confident as we further optimize this technique that we will be able to strongly trap and manipulate single digit nanometer scale particles.

In conclusion, we have shown a technique that can trap nanoscale objects using a fiber optic with no external optics. This modular fiber approach can be used to replace existing trapping setups that use bulky free space optics. Furthermore, the robustness of the cleaved fiber makes it ideal for use as a single particle nano-pipette, with the ability to trap, manipulate, and interrogate single nanoparticles and their interactions with the environment. This could lead to advances in drug discovery and our understanding of biological interactions.

References

1. X. D. Wang and O. S. Wolfbeis, Anal. Chem. **85**, 487 (2013).
2. A. Leung, P. M. Shankar, and R. Mutharasan, Sens. Actuators B **125**, 688 (2007).
3. B. Lee, Opt. Fiber Technol. **9**, 57 (2003).
4. Y. Cui, Q. Q. Wei, H. K. Park, and C. M. Lieber, Science **293**, 1289 (2001).
5. R. M. Gelfand, L. Bruderer, and H. Mohseni, Opt. Lett. **34**, 1087 (2009).
6. Y. Pang, H. Song, J. H. Kim, X. Hou, and W. Cheng, Nat. Nanotechnol. **9**, 624 (2014).
7. E. J. Smythe, M. D. Dickey, J. M. Bao, G. M. Whitesides, and F. Capasso, Nano Lett. **9**, 1132 (2009).
8. A. K. Sharma, R. Jha, and B. D. Gupta, IEEE Sens. J. **7**, 1118 (2007).
9. M. T. Myaing, D. J. MacDonald, and X. D. Li, Opt. Lett. **31**, 1076 (2006).
10. M. Kirsch, G. Schackert, R. Salzer, and C. Krafft, Anal. Bioanal. Chem. **398**, 1707 (2010).
11. L. F. Santos, R. Wolthuis, S. Koljenovic, R. M. Almeida, and G. J. Puppels, Anal. Chem. **77**, 6747 (2005).
12. M. Bowden, L. N. Song, and D. R. Walt, Anal. Chem. **77**, 5583 (2005).
13. P. Polynkin, A. Polynkin, N. Peyghambarian, and M. Mansuripur, Opt. Lett. **30**, 1273 (2005).
14. Y. Pang and R. Gordon, Nano Lett. **12**, 402 (2012).
15. A. Kotnala and R. Gordon, Nano Lett. **14**, 853 (2014).
16. A. Kotnala, D. DePaoli, and R. Gordon, Lab Chip **13**, 4142 (2013).
17. M. L. Juan, R. Gordon, Y. J. Pang, F. Eftekhari, and R. Quidant, Nat. Phys. **5**, 915 (2009).
18. A. Kotnala and R. Gordon, Biomed. Opt. Express **5**, 1886 (2014).
19. A. A. Al Balushi and R. Gordon, ACS Photonics **1**, 389 (2014).
20. J. Berthelot, S. S. Acimovic, M. L. Juan, M. P. Kreuzer, J. Renger, and R. Quidant, Nat. Nanotechnol. **9**, 295 (2014).
21. A. El Eter, N. M. Hameed, F. I. Baida, R. Salut, C. Filiatre, D. Nedeljkovic, E. Atie, S. Bole, and T. Grosjean, Opt. Express **22**, 10072 (2014).
22. P. Lambelet, A. Sayah, M. Pfeffer, C. Philipona, and F. Marquis-Weible, Appl. Opt. **37**, 7289 (1998).